Synthesis, crystal structure, and magnetic properties of MgPr9Mo16O35 – structural comparison with the LiR9Mo16O35 (R = La, Ce, Pr, Nd)

Patrick Gougeon, Philippe Gall

Synthesis, crystal structure, and magnetic properties of $MgPr_9Mo_{16}O_{35}$ – structural comparison with the $LiR_9Mo_{16}O_{35}$ (R = La, Ce, Pr, Nd)

Philippe Gall, and Patrick Gougeon*

Institut des Sciences Chimiques de Rennes, UMR 6226 CNRS – Université de Rennes 1 – INSA de Rennes, 11 allée de Beaulieu, CS 50837, 35708 Rennes Cedex, France

*Corresponding author : patrick.gougeon@univ-rennes1.fr
Tel : + 33 2 23 23 62 54
Fax : + 33 2 23 23 67 99

Abstract

Polycrystalline and single crystal specimens of the new quaternary phase $MgPr_9Mo_{16}O_{35}$ were synthesized by direct solid-state reaction. $MgPr_9Mo_{16}O_{35}$ presents a monoclinic unit cell (S.G. C2/m; a = 18.3422 (3) Å, b = 8.6188 (1) Å, c = 9.7276 (4) Å, β = 101.9680 (4) and Z = 2). Its crystal structure was solved on a single-crystal by X-ray diffraction and refined to the final values $R_1 = 0.0281$ and $wR_2 = 0.0473$ (3903 independent reflections and 101 variables). For a comparative study the crystal structure of $LiPr_9Mo_{16}O_{35}$ was also determined (a = 18.3422 (3) Å, b = 8.6188 (1) Å, c = 9.7276 (4) Å, β = 101.9680 (4) and Z = 2; $R_1 = 0.0281$ and $wR_2 = 0.0473$). The crystal structure of both compounds is based on $Mo_{16}O_{26}O_{10}$ units containing Mo_{16} clusters that share some of their O atoms to form infinite Mo-O cluster chains developing in the [010] direction and between which the Mg^{2+} or Li^{+} and Pr^{3+} cations are located. The increase of the charge transfer towards the Mo_{16} cluster due to the supplementary electron brought by the Mg^{2+} cations leads to some variations of the Mo-Mo distances. Application of the Mo-O bond-length–bond-strength relationship developed by Brown & Wu leads to a value of 55.1 electrons per Mo_{16} cluster in good agreement with that calculated from the stoichiometry (55 e^-/Mo_{16}). Magnetic susceptibility measurements confirm the presence of one unpaired electron on the Mo_{16} cluster.

Keywords

Reduced molybdenum oxides, molybdenum cluster, praseodymium, magnesium, magnetic susceptibility.

INTRODUCTION

In a previous paper, we described the series of the monoclinic compounds $LiLn_9Mo_{16}O_{35}$ (Ln = La, Ce, Pr and Nd) [1] containing the new Mo_{16} cluster. This latter can be seen as resulting from the condensation of two bi-octahedral Mo_{10} clusters [2-9] or as a fragment of the twin chain occurring in $Mn_{2.4}Mo_6O_9$.[10]. Molecular and periodic calculations based on the method EHT and carried out on the cluster $Mo_{16}O_{36}$ using experimental structural data of $LiLa_9Mo_{16}O_{35}$ allowed to highlight the existence of a favorable count of 54 electrons per Mo_{16} cluster, with a significant HOMO / LUMO gap of 0.57 eV. The molecular character of the compound is characterized by the absence of inter-clusters interactions. The periodic density functional theory confirmed the properties of semi-conductivity waited for this compound. However, although a forbidden band is calculated for the experimental metal electron count of 54, the DFT lowest vacant bands show some Mo···Mo bonding character. This indicates that metal–metal bonding in the $Mo_{16}O_{36}$ unit is optimized for an metal electron count slightly higher than the experimental one. This suggests that it should be possible to reduce the compounds $LiLn_9Mo_{16}O_{35}$. Consequently, we tried to substitute lithium for a small divalent cation that accepts a tetrahedral oxygen environment such as Mg, V, Cr, Mn, Fe, Co, Ni or Zn. Ours studies have led to the synthesis of the new compound $MgPr_9Mo_{16}O_{35}$ in which the Mo_{16} have 55 electrons. We present in this article the synthesis, crystal growth and crystal structure of this quaternary compound. The evolution of the crystal structure and in particular, the effect of adding one electron on the Mo_{16} cluster is discussed based on the variations the Mo-Mo distances. The latter ones are compared with those observed in $LiPr_9Mo_{16}O_{35}$ the crystal of which was also determined.

EXPERIMENTAL

Synthesis and Crystal Growth

Starting reagents used for the syntheses were Pr_6O_{11}, MoO_3, and Mo, all in microcrystalline form powders. Prior to use the Mo powder was reduced under a dihydrogen stream at the temperature of 1000°C during 6 hours and the rare earth oxides were heated at 1000° C overnight and left at 800°C before handling.

Single crystals of $MgPr_9Mo_{16}O_{35}$ were obtained in a reaction with the nominal composition "$MgPr_2Mo_4O_8$" heated at 1750°C for 5 mn in a sealed molybdenum crucible. Subsequently, X-ray diffractometrically pure powders of $MgPr_9Mo_{16}O_{35}$ were prepared from the required stoichiometric mixtures of the starting reagents. The mixtures were pressed into pellets (ca. 5g) and loaded into molybdenum crucibles which were previously outgassed at about 1500 °C for 15 min under a dynamic vacuum of about 10^{-5} Torr. The Mo crucibles were subsequently sealed under a low argon pressure using an arc-welding system. The samples were heated at a rate of 300°C/hour to 1400 C, kept at the temperature for 48 hours and then cooled at 100°C/hour down to 1100°C at which point the furnace was shut down and allowed to cool to room temperature. The resulting product was found to be single-phase on the basis of its X-ray powder diffraction pattern carried out on D8 Bruker Advance diffractometer equipped with a LynxEye detector ($CuK\alpha_1$ radiation) (Figure 1). In order to study the influence of the replacement of Li by Mg on the crystal structure, we also prepared single crystals of $LiPr_9Mo_{16}O_{35}$. The latter were obtained from a mixture of Li_2MoO_4, Pr_6O_{11}, MoO_3 and Mo with the overall stoichiometry "$Li_2PrMo_6O_{12}$". Li_2MoO_4 was prepared from an equi-molar ratio of Li_2CO_3 (Rhône-Poulenc, 99 %) and MoO_3 heated in air at 600°C for 12h. The crucibles were heated at a rate of 300 °Ch-1 to 1750°C and held there for 3 days, then cooled

at 100 °Ch-1 to 1100 °C and finally furnace cooled to room. The crystals grew in the form of black needles with approximately rhomboidal cross section with the needle axis parallel to the monoclinic c-axis.

While we could synthetize $Mg_{0.5}Pr_9Mo_{16}O_{35}$, attempts to get $MgLn_9Mo_{16}O_{35}$ or $Mg_{0.5}Ln_9Mo_{16}O_{35}$ compounds with Ln = La, Ce, and Nd were unsuccessful. On the other hand, an isostructural phase was observed with the zinc. However, we were unable to obtain a monophasic powder or single crystals of the latter compound.

Single Crystal X-ray Study

The X-ray diffraction data for $LiPr_9Mo_{16}O_{35}$ and $MgPr_9Mo_{16}O_{35}$ were collected on a Nonius Kappa CCD diffractometer using graphite-monochromated Mo-Kα radiation (λ = 0.71073 Å) at room temperature. The COLLECT program package [11] was employed to establish the angular scan conditions (φ and ω scans) used in the data collection. The data set was processed using EvalCCD [12] for the integration procedure. An absorption correction was applied using the description of the crystal faces and the analytical method described by de Meulenaar and Tompa [13]. Analysis of the data revealed that the systematic absences were consistent with the monoclinic space group C2/m. The structure was solved with the direct methods program SIR97 [14] and refined using SHELXL97 [15]. Crystallographic data and X-ray structural analysis for both compound are summarized in Table 1, and selected interatomic distances are listed in Table 2. Further details of the crystal structure investigation can be obtained from the Fachinformationszentrum Karlsruhe, 76344 Eggenstein-Leopoldshafen, Germany, (fax: (49) 7247-808-666; e-mail: crysdata@fiz.karlsruhe.de) on quoting the depository number CSD- 419443.

Magnetic susceptibility measurements.

Susceptibility data were collected on cold pressed powder samples (ca. 100 mg) using a Quantum Design SQUID magnetometer between 2 K and 400 K and at an applied field of 0.1 T.

RESULTS AND DISCUSSION

Crystal Structure

The unit cell parameters of $MgPr_9Mo_{16}O_{35}$ and $LiPr_9Mo_{16}O_{35}$ are summarized in Table 1. As shown by the figures 2, the unit cell parameters of $MgPr_9Mo_{16}O_{35}$ do not follow the general trends observed for the lithium phases $LiR_9Mo_{16}O_{35}$. Indeed, the replacement of Li by Mg leads to an increase of the a parameter and a decrease of the c parameter while the b parameter and the β angle are almost similar in both phases. The overall effect is a slight increase of the unit cell volume of the Mg phase.

$MgPr_9Mo_{16}O_{35}$ and $LiPr_9Mo_{16}O_{35}$ are isotopic with the $LiNd_9Mo_{16}O_{35}$ structure type that was first described in 2011. The crystal structure is based on $Mo_{16}O_{26}{}^{i}O_{10}{}^{a}$ cluster units (Fig. 3) sharing two O^i or four O^a ligands (for details of the i- and a-type ligand notation, see Schäfer & von Schnering [16]) to form infinite molybdenum cluster chains running paralelly to the b axis (Figs. 4 and 5). The Mo_{16} core of the unit can be seen as resulting of the fusion of two bioctahedral Mo_{10} clusters through the sharing of three edges per Mo_{10} cluster (Fig. 6 center). The Mo_{10} cluster results itself from metal edge-sharing of two Mo_6 octahedral (Fig. 6 left) and was first observed forming infinite chain in the MMo_5O_8 (M =Ca, Sr, Sn, Pb, La-Gd) compounds [2-8] and more latter as isolated cluster in the $R_{16}Mo_{21}O_{56}$ (R = La, Ce, Pr, and Nd) series [9]. Examination of the Mo-Mo and Mo-O distances in table 2 shows that the replacement of the Li by the Mg atom induce some variations. Indeed, for the Mo-Mo bonds, the greatest differences are observed for the Mo5-Mo5 and Mo2-Mo2 bonds whose the length

increases by 0.037 and 0.018 Å, respectively, while the other differences do not exceed 0.014 Å. For the Mo-O bonds, the greatest variations concern the Mo4-O10 and Mo2-O7 bonds the lengths of which undergo an augmentation of 0.041 and 0.034 Å, respectively. This results probably from the replacement of the Li^+ by the Mg^{2+} cations since both oxygen atoms form their octahedral environment. Indeed, the Mg^{2+} cation as Li^+ occupies a highly tetragonally distorted octahedral site of O atoms of symmetry 2/m centered at the origin of the unit cell. The Mg—O distances in the equatorial plane are 2.317 (2) Å [Mg—O10] and the two trans Mg—O7 bonds are 1.920 (3) Å. In $LiPr_9Mo_{16}O_{35}$, these two bonds are equal to 2.3979(19) and 1.859(3) Å, respectively. The coordination numbers of the Pr ions are 6, 7, 9 or 10 with Pr—O distances spreading over a wide range [2.24 to 2.96 Å]. By using the bond-length–bond-strength formula developed by Brown & Wu [17] for the Mo—O, Pr-O, Mg—O and Li—O bonds ($s = [d(Mo—O)/1.882]^{-6}$, $s = [d(Pr—O)/2.150]^{-6.5}$, $s = [d(Mg—O)/1.622]^{-4.29}$ and $s = [d(Li—O)/1.378]^{-4.065}$), an assignment of oxidation states to the Mo, Pr, Mg and Li atoms was made. All these values are reported in Table 3. For the Mo atoms, we could deduce a number of electrons of 55.1 and 54.4 in the Mg and Li compounds, respectively. Both values are close to those based on the stoichiometry, 55 and 54, when considering all the Pr ions as trivalent, the Mg as divalent and the Li ion monovalent. Bond-valence sums of the Pr—O bonds confirm the trivalent state of the praseodymium. For the Li and Ca atoms, values of +1.01 ans 1.85 were found. It is interesting to note that for the total valence sum Σ(Mo—O) + Σ(Ce—O) + Σ(Li—O), we obtained a value of 70.5 per formula unit, which is in very good agreement with the theoretical value of 70 based on the 35 O atoms.

Magnetic Properties.

The molar magnetic susceptibility data for $MgPr_9Mo_{16}O_{35}$ and $Mg_{0.5}Pr_9Mo_{16}O_{35}$ have been measured between 2 and 300 K on powder samples. Their inverse of their susceptibility as well as that of $LiPr_9Mo_{16}O_{35}$, previously published in Ref. 1, as a function of the temperature is shown in Figure 7. As evidenced from the figure 7, the compounds $LiPr_9Mo_{16}O_{35}$ and $Mg_{0.5}Pr_9Mo_{16}O_{35}$ in which the Mo_{16} clusters have 54 e^- present a very similar behaviour with an effective moment of 3.459 and 3.462 μ_B per Pr^{3+} ion obtained by fitting the $1/\chi$ vs T curves to a modified Curie-Weiss like behaviour $\chi = C/(T-\theta) + \chi_0$ in the temperature range 120-300 K. $MgPr_9Mo_{16}O_{35}$ in which the Mo_{16} clusters have 55 e^-, has a higher effective moment per Pr^{3+} ion of 3.5 μ_B. For $LiPr_9Mo_{16}O_{35}$ and $Mg_{0.5}Pr_9Mo_{16}O_{35}$, the negative Weiss temperatures suggest that the exchange correlations are antiferromagnetic, although no magnetic ordering was evident down to 2 K. An almost constant susceptibility of about 0.5 and was also observed for $Mg_{0.5}Pr_9Mo_{16}O_{35}$ as previously observed for the Li compound below 8 K indicating a non-magnetic single ground state as expected from the non-Kramer nature of the Pr^{3+} ions ($^3H_4$ ground state) and the low symmetry of the Pr^{3+} sites [18-20]. Below 50 K, the 1/x vs. temperature curve of $MgPr_9Mo_{16}O_{35}$ deviates from the curie Weiss law. Evidence for long range magnetic order at low temperatures is seen in Figure 8 showing the ZFC and FC curves. An inflection point is clearly seen both in χ versus T and $1/\chi$ versus T plots at about 25 K. The shape of the χ versus T curve is characteristic of ferromagnetism or weak ferro-magnetism. Such behaviour does not arise from impurities since $Mg_{0.5}Pr_9Mo_{16}O_{35}$ that was synthesized from the same starting reactants and the same time do not present this behaviour. This behaviour recalls that of the compound $NdMo_8O_{14}$ [21] containing Mo_8 clusters with 23 electrons that also presents the characteristics of a ferromagnetic or a weak ferromagnetic compound. In solid-state compounds, only few examples reported in the literature have provided evidence that magnetic cluster–cluster interactions can be strong enough to reach a long-range ordering of unpaired spins. For example, antiferromagnetic interactions between

$[Nb_6Cl_{12}]^{3+}$ cluster cores were clearly evidenced in the $LuNb_6Cl_{18}$ compound that was crystallographically and magnetically characterised [22]. More recently, temperature-dependent ^{19}F NMR spectroscopic and EPR measurements of the Nb_6F_{15} compound revealed also antiferromagnetic interactions between $[Nb_6F_{12}]^{3+}$ cluster cores [23]. Ferromagnetic interactions have also been reported for the $GaMo_4X_8$ (X = S, Se) compounds [24] containing tetrahedral Mo_4 clusters with 11 electrons.

CONCLUSION

In agreement with previous periodic DFT calculation on $LiLa_9Mo_{16}O_{35}$ that, although a forbidden band calculated for the experimental metal electron count of 54, show that the Mo-Mo connection in the Mo_{16} cluster is optimized for a count of electrons upper to this experimental count, we could synthesize the new compound $MgPr_9Mo_{16}O_{35}$ in which the Mo_{16} have 55 electrons. The increase of the charge transfer towards the Mo_{16} cluster due to the supplementary electron brought by the Mg^{2+} cations leads to some variations of the Mo-Mo distances within the Mo_{16} cluster. Application of the Mo-O bond-length–bond-strength relationship developed by Brown & Wu leads to a value of 55.1 electrons per Mo_{16} cluster and thus confirmed that deduced from the stoichiometry of 55 e^-/Mo_{16}. Magnetic susceptibility measurements confirm the presence of one unpaired electron on the Mo_{16} cluster with a slightly higher effective moment per Pr^{3+} ion than those observed for $LiPr_9Mo_{16}O_{35}$ and $Mg_{0.5}Pr_9Mo_{16}O_{35}$. In addition, $MgPr_9Mo_{16}O_{35}$ presents a long range magnetic order below 25 K arising probably from a ferromagnetic or weak ferromagnetic ordering.

References

[1] P. Gougeon, P. Gall, J. Cuny, R. Gautier, L. Le Polles, L. Delevoye, J. Trebosc, Synthesis, Crystal and Electronic Structures, and Magnetic Properties of $LiLn_9Mo_{16}O_{35}$ (Ln=La, Ce, Pr, and Nd) Compounds Containing the Original Cluster $Mo_{16}O_{36}$, Chemistry-a European Journal 17(49) (2011) 13806-13813.

[2] S.J. Hibble, A.K. Cheetham, A.R.L. Bogle, H.R. Wakerley, D.E.J. Cox, The Synthesis and Structure Determination From Powder Diffraction Data of $LaMo_5O_8$ A New Oxomolybdate Containing Mo10 Clusters, Am. Chem. Soc. 110 (1988) 3295-3296

[3] R. Dronskowski, A. Simon, $PbMo_5O_8$ and $Tl_{0.8}Sn_{0.6}Mo_7O_{11}$, Novel Clusters of Molybdenum and Thallium, Angew. Chem. Int. Ed. Engl. 28 (1989) 758-760.

[4] P. Gougeon, M. Potel, M. Sergent, Structure of $SnMo_5O_8$ Containing Bioctahedral Mo_{10} Clusters, Acta Crystallographica Section C-Crystal Structure Communications 46 (1990) 1188-1190.

[5] P. Gougeon, P. Gall, M. Sergent, Structure of $GdMo_5O_8$, Acta Crystallographica Section C-Crystal Structure Communications 47 (1991) 421-423.

[6] R. Dronskowski, A. Simon, W. Mertin, Synthesis and Crystal-Structure of $PbMo_5O_8$ - A Reduced Oxomolybdate with $Mo_{10}O_{28}$ Double Octahedra, Z. Anorg. Allg. Chem. 602 (1991) 49-63.

[7] P. Gall, P. Gougeon, Structure of $SrMo_5O_8$ Containing Chains of Bioctahedral Mo_{10} Clusters, Acta Crystallographica Section C-Crystal Structure Communications 50 (1994) 7-9.

[8] P. Gall, P. Gougeon, Redetermination of The Structure of $LaMo_5O_8$ By Single-Crystal X-Ray-Diffraction, Acta Crystallographica Section C-Crystal Structure Communications 50 (1994) 1183-1185.

[9] P. Gall, R. Gautier, J.F. Halet, P. Gougeon, Synthesis, physical properties, and theoretical study of $R_{16}Mo_{21}O_{56}$ compounds (R = La, Ce, Pr, and Nd) containing bioctahedral Mo_{10} clusters and single Mo atoms, Inorganic Chemistry 38(20) (1999) 4455-4461.

[10] N. Barrier, P. Gougeon, R. Retoux, H. Leligny, $Mn_{2.4}Mo_6O_9$: First example of empty twin chains of edge-sharing M_6 octahedra in transition metal cluster chemistry, Inorganic Chemistry 42(5) (2003) 1734-1738.

[11] Nonius BV, COLLECT, Data Collection Software, Nonius BV, 1999.

[12] A. J. M. Duisenberg, Reflections on area detectors, Ph.D. Thesis, Utrecht, 1998.

[13] J. de Meulenaar, H. Tompa, The Absorption Correction in Crystal Structure Analysis., Acta Crystallogr., Sect. A: Found. Crystallogr. 19 (1965) 1014.

[14] A. Altomare, M. C. Burla, M. Camalli, G. L. Cascarano, C. Giacovazzo, A. Guagliardi, A. G. G. Moliterni, G. Polidori, R. Spagna, SIR97: a new tool for crystal structure determination and refinement, J. Appl. Cryst. 32 (1999) 115.

[15] G. M. Sheldrick, SHELXL97, Program for the Refinement of Crystal Structures, University of Göttingen, Germany, 1997.

[16] H. Schäfer, H. G. Von Schnering, Metall-Metall-Bindungen bei Niederen Halogeniden, Oxyden und Oxydhalogeniden Schwerer Übergangsmetalle Thermochemische und Strukturelle Prinzipien. Angew. Chem. 20 (1964) 833–849.

[17] I.D. Brown and K.K. Wu, Empirical Parameters for Calculating Cation-Oxygen Bond Valences. Acta Crystallogr. B32 (1976) 1957-1959.

[18] J. H. Van Vleck, Electric and Magnetic Susceptibilities, Oxford University Press, New York, 1932, p. 243..

[19] Kramers, H. A., General theory of the paramagnetic rotation in crystals, Proceedings of The Koninklijke Akademie Van Wetenschappen Te Amsterdam. 1930, 33,959-972.

[20] E. F. Bertaut, Survey of Magnetism In Solid-State Chemistry 1966-1975, Ann. Chim. 1976, 1, 83-99.

[21] R. Gautier, O. Krogh Andersen, P. Gougeon, J.-F. Halet, E. Canadell, J. D. Martin, Electronic structure, electrical and magnetic properties of RMo_8O_{14} compounds (R = La, Ce, Pr, Nd, Sm) containing bicapped Mo_8 clusters. Inorg. Chem. 41 (2002) 4689-4699.

[22] S. Ihmaïne, C. Perrin, O. Pena, M. Sergent, Structure and magnetic-properties of 2 niobium chlorides with $(Nb_6Cl_{12})^{N+}$ (N=2, 3) units - $KLuNb_6Cl_{18}$ and $LuNb_6Cl_{18}$. J. Less-Common Met. 137 (1988) 323 –332.

[23] R. Knoll, J. Sokolovski, Y. BenHaim, A. I. Shames, S. D. Goren, H. Shaked, J.-Y. Thépot, C. Perrin, S. Cordier, Magnetic resonance and structural study of the cluster fluoride Nb_6F_{15}. Physica B 381 (2006) 47–52.

[24] H. Ben Yaich, J. C. Jegaden, M. Potel, R. Chevrel, M. Sergent, A. Berton, J. Chaussy, A. K. Rastogi, R. Tournier, $GaMo_4(XX')_8$ (X=S, Se, Te) new mixed chalcogenides with Mo_4 tetrahedral clusters. J. of Solid State Chem. 51 (1983) 212-217.

Table Captions:

Table 1. Crystal data and structure refinements of $MgPr_9Mo_{16}O_{35}$ and $LiPr_9Mo_{16}O_{35}$.

Table 2. Selected Interatomic Distances for $LiPr_9Mo_{16}O_{35}$ and $MgPr_9Mo_{16}O_{35}$.

Table 3. Oxidation states of the Mo, Pr, Mg and Li atoms deduced from the bond-length–bond-strength formula developed by Brown & Wu.

Figure Captions

Figure 1. Observed (dotted line), calculated (red line) and difference profiles for the refinement of $MgPr_9Mo_{16}O_{35}$ in profile-matching mode (λ = 1.5406 Å).

Figure 2. Variations of (a) the *a*, *b*, *c* and (b) β cell parameters as a function of the rare-earth for the $MR_9Mo_{16}O_{35}$ (M = Li, Mg; R = La, Ce, Pr, and Nd) compounds.

Figure 3. The Mo_{16} cluster with its oxygen environment.

Figure 4. The crystal structure of $MgPr_9Mo_{16}O_{35}$ as viewed down the c axis. Ellipsoids are drawn at the 97 % probability level.

Figure 5. The crystal structure of $MgPr_9Mo_{16}O_{35}$ as viewed down the b axis. Ellipsoids are drawn at the 97 % probability level.

Figure 6. Formation of the Mo_{16} cluster.

Figure 7. Reciprocal susceptibility of $LiPr_9Mo_{16}O_{35}$ and $MgPr_9Mo_{16}O_{35}$ as a function of temperature. Data were taken under an applied field of 0.1 T. The solid line represents the fit to a modified Curie-Weiss law in the range of 300-400K.

Figure 8. FC and ZFC curve for $MgPr_9Mo_{16}O_{35}$.

Table 1. Crystal data and structure refinements of $MgPr_9Mo_{16}O_{35}$ and $LiPr_9Mo_{16}O_{35}$

Empirical formula	$MgPr_9Mo_{16}O_{35}$	$LiPr_9Mo_{16}O_{35}$
Formula weight (g mol−1)	3387.54	3370.17
Crystal system, space group	monoclinic, C2/m	
Unit cell dimensions (Å, deg)	*a* = 18.3422 (3) *b* = 8.6188 (1) *c* = 9.7276 (2) β = 101.9680 (7)	*a* = 18.2149 (2) *b* = 8.6183 (1) *c* = 9.7772 (1) β = 101.9741 (8)
Volume (Å3)	1504.39 (4)	1501.44(3)
Z, Calculated density (g/cm3)	2, 7.478	2, 7.455
Absorption coefficient (mm−1)	20.793	20.812
Crystal color and habit	Black, multifaceted block	Black, needle like
Crystal size (mm3)	0.084 × 0.072 × 0.056	0.566 x 0.053 x 0.039
Theta range for data collection (deg)	3.53–34.995	3.53-34.984
Limiting indices	-29≤*h*≤28, -11≤*k*≤13, −15≤*l*≤15	-29≤*h*≤29, -13≤*k*≤13, −10≤*l*≤15
Reflections collected/unique	19818/3483	20062/3465
R (int)	0.0307	0.0272
Absorption correction	Analytical	Analytical
Max./min. transmission	0.4142/0.1328	0.5622/0.0425
Data/restraints/parameters	3483/0/159	3465/0/159
Goodness-of-fit on F^2	1.22	1.289
R indices [$I>2\sigma(I)$]	R1=0.0211, wR2=0.0353	R1=0.0174, wR2=0.0358
Extinction coefficient	0.000301(13)	0.00217(4)
Largest diff. peak and hole ($eÅ^{-3}$)	1.543 and −1.598	1.302 and -1.782

Table 2. Selected Interatomic Distances for $LiPr_9Mo_{16}O_{35}$ and $MgPr_9Mo_{16}O_{35}$.

	$LiPr_9Mo_{16}O_{35}$	$MgPr_9Mo_{16}O_{35}$
Pr(1)-O(3)	2.339(2)	2.3405(2)
Pr(1)-O(12)	2.3868(16)	2.3918((17)
Pr(1)-O(1)	2.3939(5)	2.3835(5)
Pr(1)-O(8)	2.4037(19)	2.3800(19)
Pr(1)-O(10)	2.5402(19)	2.623(2)
Pr(1)-O(4)	2.694(2)	2.702(2)
Pr(1)-O(2)	2.834(2)	2.794(2)
Pr(1)-O(11)	2.873(2)	2.849(2)
Pr(1)-O(7)	2.883(2)	2.862(2)
Pr(2)-O(12)	2.319(3)	2.324(3)
Pr(2)-O(3) (x2)	2.373(2)	2.365(2)
Pr(2)-O(1)	2.606(3)	2.622(3)
Pr(2)-O(2) (x2)	2.621(2)	2.617(2)
Pr(2)-O(5) (x2)	2.7924(19)	2.817(2)
Pr(2)-O(2) (x2)	2.9547(19)	2.9557(18)
Pr(3)-O(12)	2.348(3)	2.339(3)
Pr(3)-O(8) (2)	2.3545(19)	2.350(2)
Pr(3)-O(4) (x2)	2.518(2)	2.524(2)
Pr(3)-O(5) (x2)	2.7736(19)	2.7586(19)
Pr(4)-O(6) (x2)	2.257(3)	2.236(3)
Pr(4)-O(3) (x4)	2.415(2)	2.433(2)
Mo(1)-O(2) (x2)	1.977(2)	1.9837(19)
Mo(1)-O(4) (x2)	2.033(2)	2.027(2)
Mo(1)-O(1)	2.042(3)	2.041(3)
Mo(1)-Mo(3)	2.6966(3)	2.7035(4)
Mo(1)-Mo(2)	2.7110(3)	2.6989(3)
Mo(2)-O(3)	2.027(2)	2.037(2)
Mo(2)-O(7)	2.074(2)	2.108(2)
Mo(2)-O(2)	2.079(2)	2.072(2)
Mo(2)-O(5)	2.0994(19)	2.0826(19)
Mo(2)-O(10)	2.1034(19)	2.121(2)
Mo(2)-Mo(4)	2.6386(3)	2.6411(3)
Mo(2)-Mo(5)	2.7680(3)	2.7548(5)
Mo(2)-Mo(3)	2.7732(3)	2.7747(3)
Mo(2)-Mo(2)	2.7842(4)	2.8024(4)
Mo(3)-O(8)	2.0312(19)	2.0315(19)
Mo(3)-O(5)	2.0693(19)	2.073(19)
Mo(3)-O(11)	2.081(2)	2.081(2)
Mo(3)-O(4)	2.0831(19)	2.086(2)

Mo(3)-Mo(3)	2.7322(4)	2.7259(4)
Mo(3)-Mo(4)	2.7349(3)	2.7423(3)
Mo(3)-Mo(5)	2.7377(3)	2.7521(4)
Mo(3)-Mo(4)	2.8351(3)	2.8208(3)
Mo(3)-Mo(5)	2.8916(3)	2.8819(3)
Mo(4)-O(6)	2.0132(18)	2.0097(19)
Mo(4)-O(8)	2.0743(19)	2.074(2)
Mo(4)-O(5)	2.0783(19)	2.077(2)
Mo(4)-O(10)	2.0850(19)	2.126(3)
Mo(4)-O(9)	2.1115(2)	2.1204(2)
Mo(4)-Mo(5)	2.7328(2)	2.7258(2)
Mo(4)-Mo(4)	2.7955(4)	2.8095(5)
Mo(4)-Mo(4)	3.1654(4)	3.1767(4)
Mo(5)-O(11)	2.078(3)	2.078(3)
Mo(5)-O(10) (x2)	2.0932(19)	2.1109(19
Mo(5)-Mo(5)	2.9036(6)	2.9404(6)
Li/Mg-O(7) (x2)	1.859(3)	1.920(3)
Li/Mg-O(10) (x4)	2.3979(19)	2.317(2)

	$LiCe_9Mo_{16}O_{35}$	$LiPr_9Mo_{16}O_{35}$	$MgPr_9Mo_{16}O_{35}$	$LiNd_9Mo_{16}O_{35}$
Mo1	+3.36	+3.36	+3.35	+3.36
Mo2	+2.78	+2.78	+2.72	+2.78
Mo3	+2.29	+2.29	+2.28	+2.30
Mo4	+2.81	+2.82	+2.76	+2.82
Mo5	+1.60	+1.61	+1.57	+1.61
Pr1		+3.10	+3.10	
Pr2		+3.12	+3.11	
Pr3		+2.77	+2.80	
Pr4		+3.34	+3.34	
M		+1.01	+1.84	

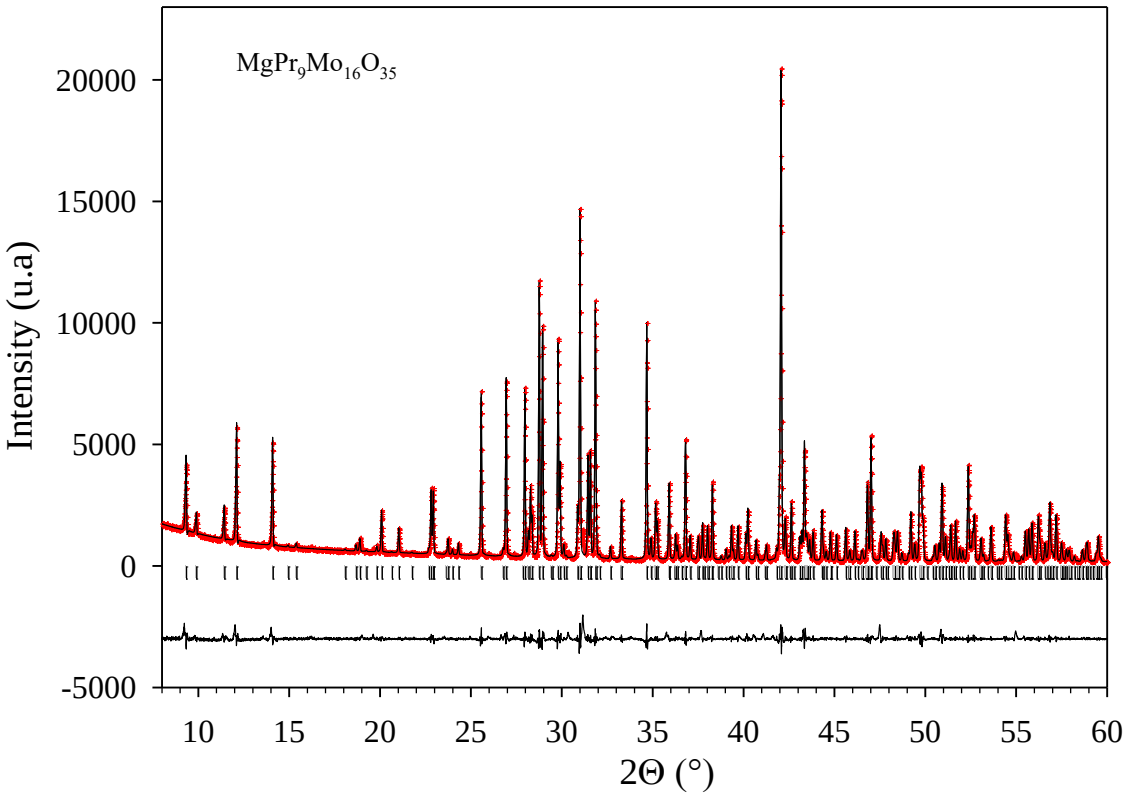

Figure 1

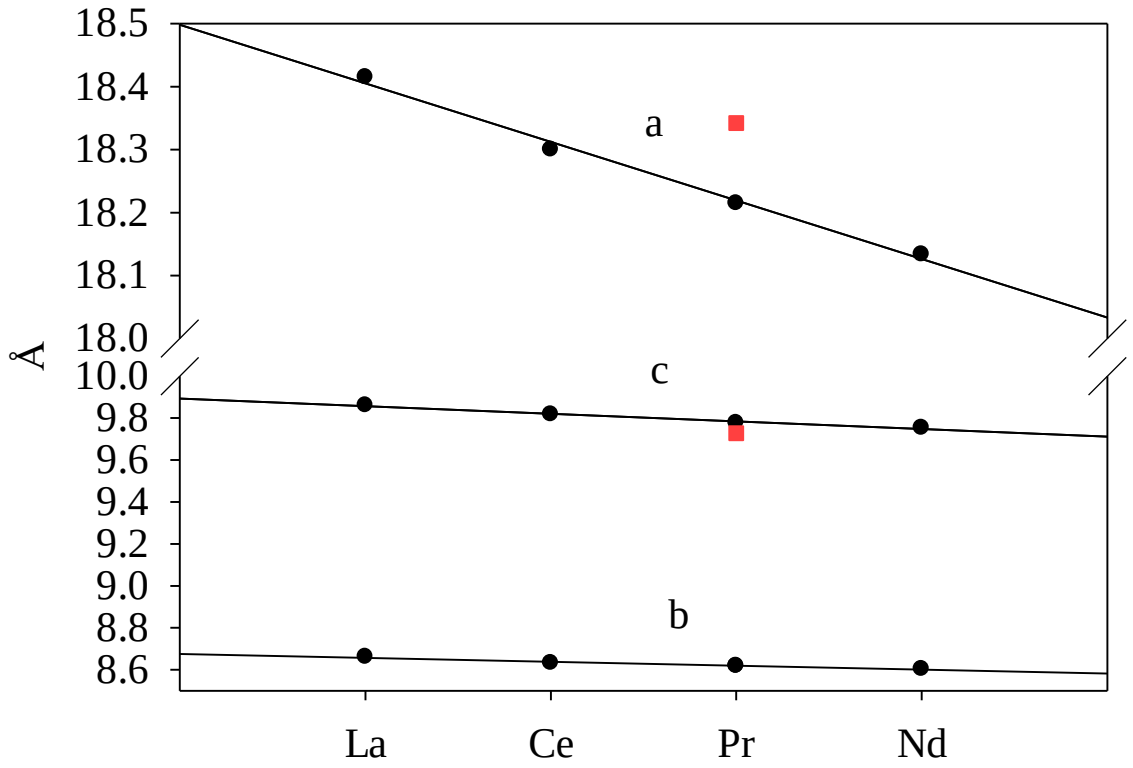

(a)

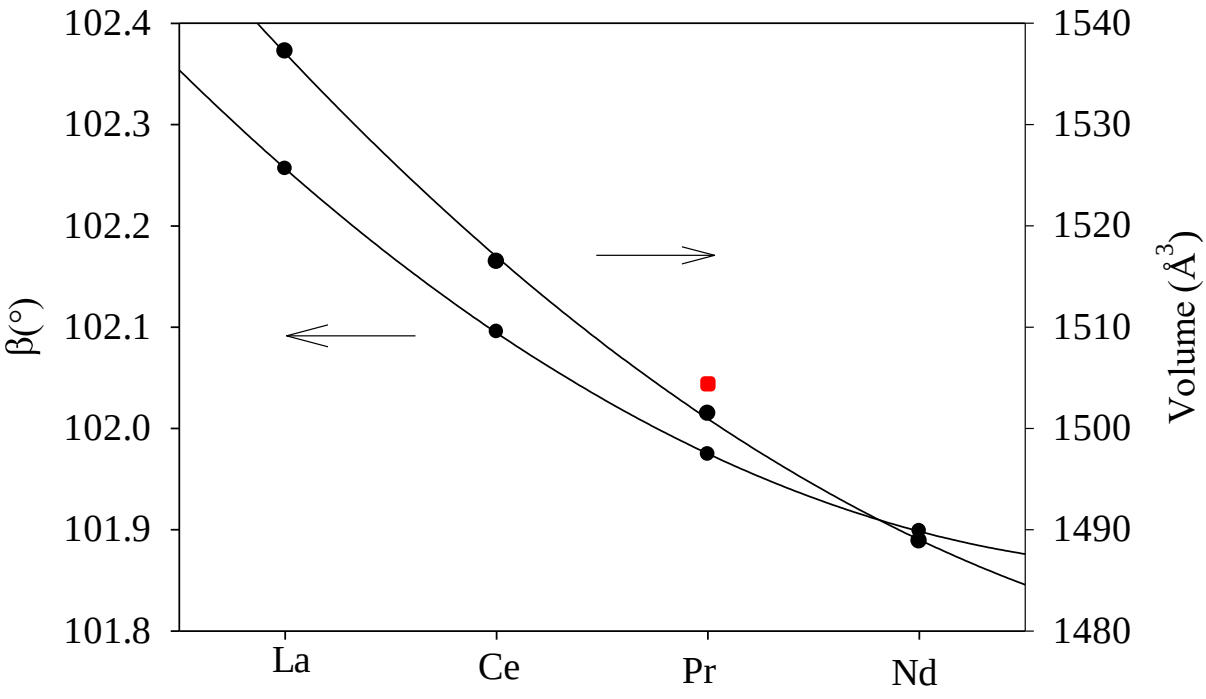

(b)

Figure 2

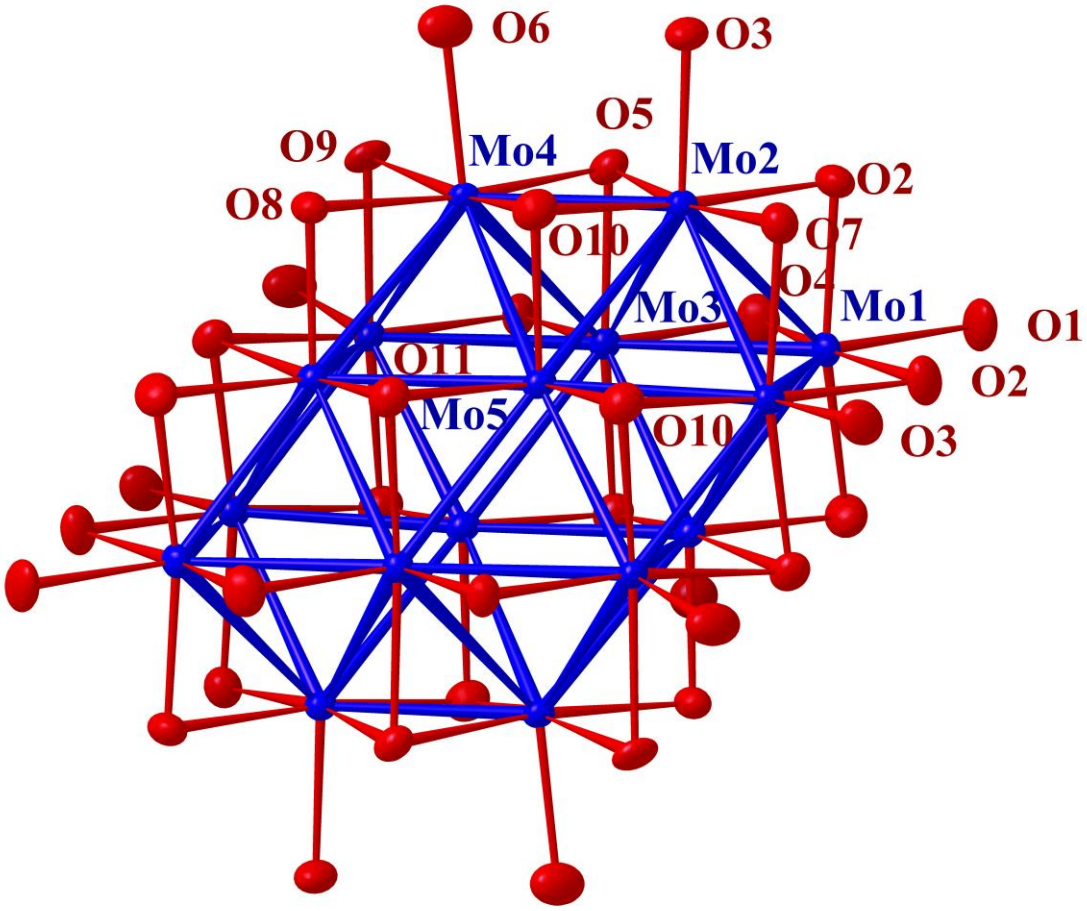

Figure 3

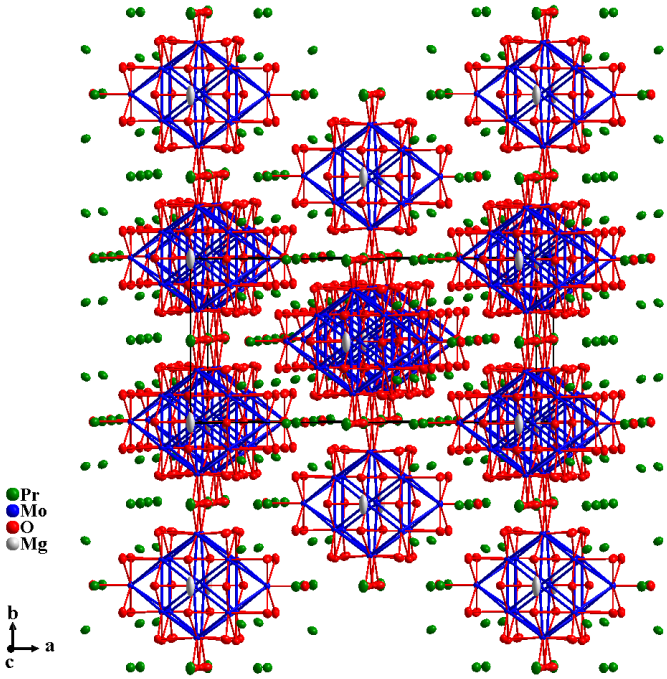

Figure 4

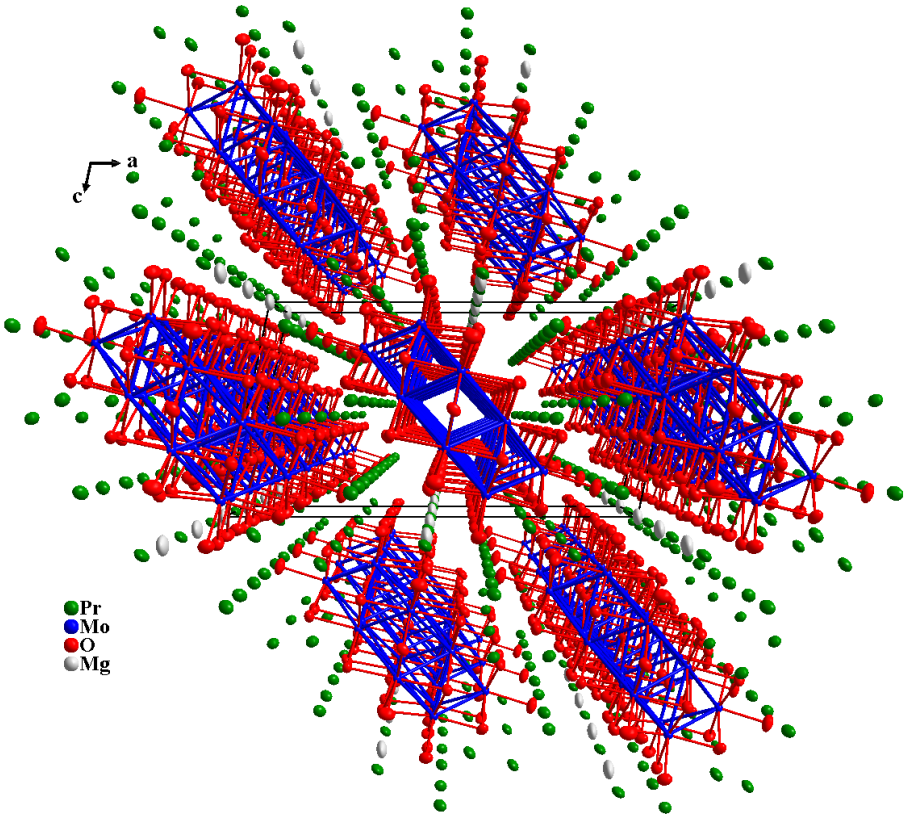

Figure 5

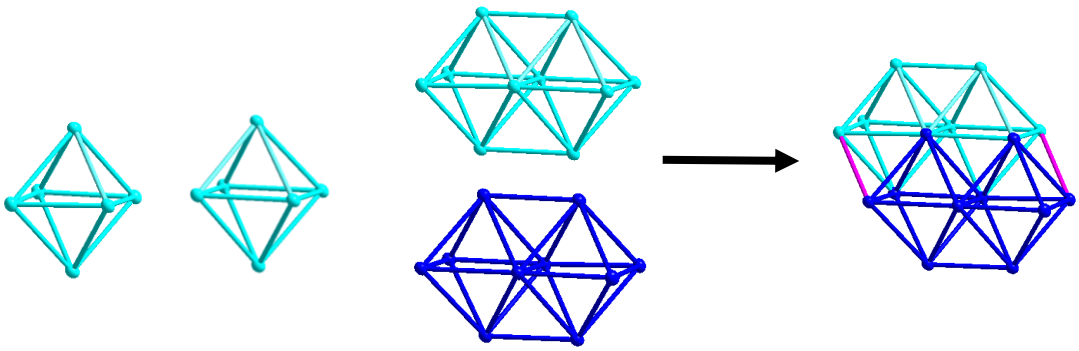

Figure 6

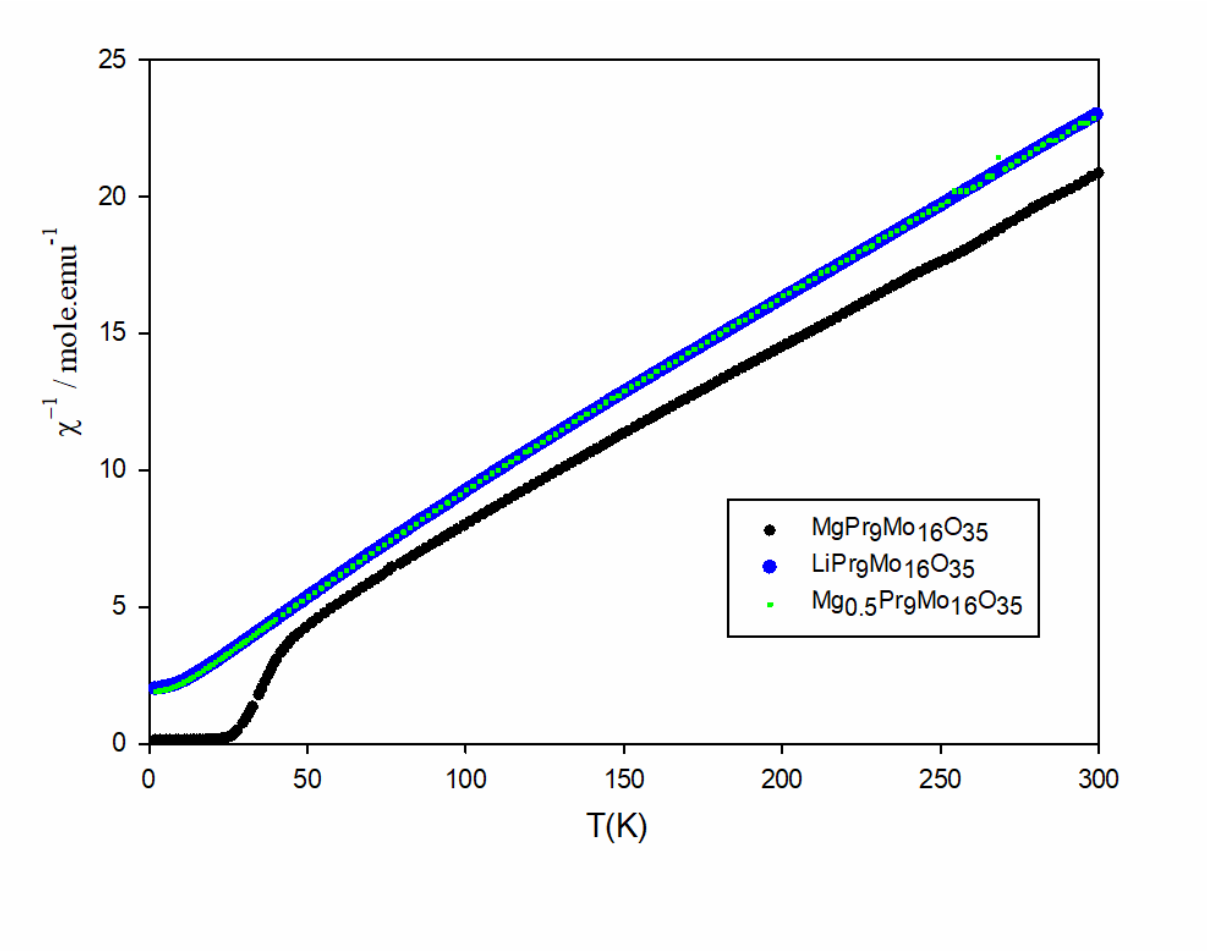

Figure 7

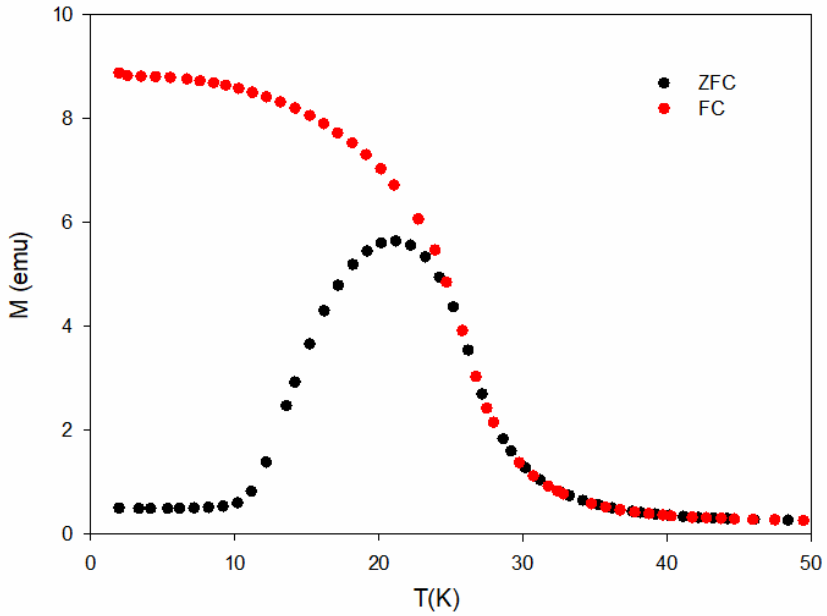

Figure 8